# SCIENTIFIC REPORTS

OPEN

Correspondence and
requests for materials
should be addressed to
D.W. (wirtz@jhu.edu)
or G.D.L. (glongmor@
dom.wustl.edu)

* Current address:
Department of
Mathematics,
University of California
Davis, Davis,
California, USA.

Actin cap associated focal adhesions and their distinct role in cellular mechanosensing

Dong-Hwee Kim[1,2], Shyam B. Khatau[1,2], Yunfeng Feng[1,3], Sam Walcott[1,4]*, Sean X. Sun[1,2,4], Gregory D. Longmore[1,3] & Denis Wirtz[1,2]

[1]Johns Hopkins Physical Sciences in Oncology Center, The Johns Hopkins University, Baltimore, Maryland 21218, USA, [2]Department of Chemical and Biomolecular Engineering, The Johns Hopkins University, Baltimore, Maryland 21218, USA, [3]Departments of Medicine and Cell Biology and Physiology, Washington University School of Medicine, St. Louis, MO 63110, USA, [4]Department of Mechanical Engineering, The Johns Hopkins University, Baltimore, Maryland 21218, USA.

The ability for cells to sense and adapt to different physical microenvironments plays a critical role in development, immune responses, and cancer metastasis. Here we identify a small subset of focal adhesions that terminate fibers in the actin cap, a highly ordered filamentous actin structure that is anchored to the top of the nucleus by the LINC complexes; these differ from conventional focal adhesions in morphology, subcellular organization, movements, turnover dynamics, and response to biochemical stimuli. Actin cap associated focal adhesions (ACAFAs) dominate cell mechanosensing over a wide range of matrix stiffness, an ACAFA-specific function regulated by actomyosin contractility in the actin cap, while conventional focal adhesions are restrictively involved in mechanosensing for extremely soft substrates. These results establish the perinuclear actin cap and associated ACAFAs as major mediators of cellular mechanosensing and a critical element of the physical pathway that transduce mechanical cues all the way to the nucleus.

During the early stages of development, immune responses, and cancer metastasis, cells negotiate continuously changing microenvironments, which differ not only in their biochemical composition, but also in their mechanical compliance. Changes in the mechanical compliance of the extracellular matrix can be sensed by adherent cells and can alone drive major cytoskeleton re-organization, protrusion dynamics[1], cellular motility (durotaxis)[2], tumor progression[3], and stem cell differentiation[4] independent of changes in ligand presentation. We distinguish mechanosensing, the ability of cells to sense changes in the compliance of their microenvironment and remodel their cytoskeleton, from mechanotransduction, the ability of cells to respond to applied mechanical stresses by changing their gene expression. Cellular mechanosensing is mediated by focal adhesions[2,5], discrete protein clusters located at the basal cellular surface of cells. Focal adhesions anchor the cell to its underlying substratum and serve as bidirectional signaling conduits between the extracellular environment and the intracellular milieu[6]. Focal adhesions terminate actomyosin stress fibers that lie at the basal cellular surface and mediate cellular adhesion to the extracellular matrix through dynamically regulated binding between clustered transmembrane adhesion molecules (integrins) and specific focal adhesion proteins. Cells *in vitro* and *in vivo* apically polarized and positioned on 2D extracellular matrix readily form focal adhesions. More than 100 focal adhesion-specific proteins have been identified[7], including enzymes (e.g. focal adhesion kinase, FAK[8]), scaffolding proteins (e.g. paxillin[9]), adaptor proteins (e.g. zyxin[10]), structural proteins (e.g. talin[11,12]), F-actin binding proteins (e.g. α-actinin[13–15]), and integrin linker proteins (e.g. talin[12]), which mediate inside-out and outside-in signaling, micro-environmental sensing[16], and coordinated cell migration[16,17].

Here we show that early mechanosensing is dominated by a small and distinct subset of actin filaments and their associated focal adhesions and not by conventional stress fibers that terminate at conventional focal adhesions. These unique actin filaments form highly organized, oriented, thick bundles that tightly cover the apical surface of the nucleus in adherent cells to form the perinuclear actin cap (Fig. 1A and Suppl. Movie 1)[18,19]. The actin cap is composed of contractile actomyosin filament bundles that continuously bend to cover the top of the nucleus, as opposed to lying flat at the basal surface of the cell like conventional basal stress fibers[18,19]. Actin cap fibers are also distinct from dorsal or radial stress fibers, which generate at the ventral surface of certain cell lines including U2OS cells[20–22], rise towards the dorsal surface of the cell, and terminate at transverse arcs (see more details below). Unlike conventional stress fibers, actin cap fibers are directly connected to the nuclear
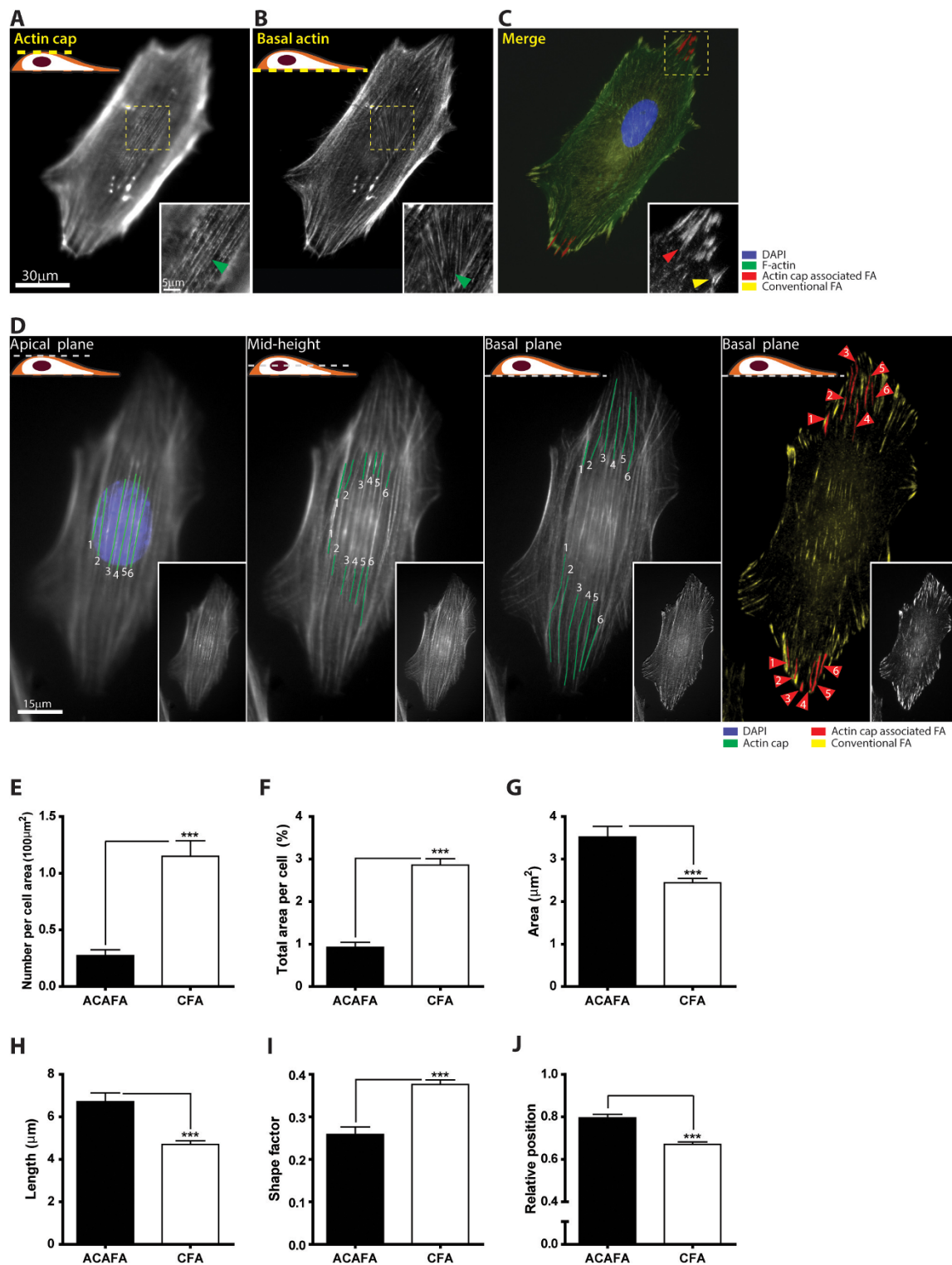
Figure 1 | Actin cap associated focal adhesions (ACAFAs) – differences with conventional focal adhesions (CFAs). Organization of actin filaments and focal adhesions in a mouse embryonic fibroblast (MEF). (A) Focus on the top of the nucleus reveals highly ordered fibers forming the perinuclear actin cap. *Inset*, detail of the highly ordered actin fibers. The arrowhead indicates an actin cap fiber. (B) Focus on the basal surface of the cell shows conventional basal stress fibers. *Inset*, organization of F-actin underneath the nucleus. (C) F-actin (green), conventional focal adhesions (yellow) terminating the actin fibers lying in the basal cell layer, actin cap associated focal adhesions (red) terminating the actin cap fibers, and nucleus (DAPI, blue). Focal adhesions are visualized with an anti-vinculin. *Inset*, ACAFA (red arrow head) and conventional focal adhesion (yellow arrow head). (D) Progressive lowering of the focal plane from the apical surface of a cell to its basal surface shows how ACAFAs are defined as the subset of focal adhesions terminating actin fibers wrapping around the nucleus. All the other focal adhesions are termed conventional focal adhesions (CFAs). The parts of the bundles that are in focus are in green. Numbering of the actin cap fibers shows the corresponding actin cap associated focal adhesions. *Insets*, unlabelled stress fibers in the region of interest. (E–J) ACAFAs and CFAs display significantly different number per unit area of cell (E), fraction of the cell surface area occupied by focal adhesions (F), surface area per focal adhesion (G), their length (H), shape factor (I), and relative subcellular position between the cell periphery and the center of the cell (J). For condition in panels E and F, at least 30 cells were analyzed and 300 focal adhesions for each condition in panels G–J. ***: $P < 0.001$.

envelope[18] through linkers of nucleoskeleton and cytoskeleton (LINC) complexes[23]. Indeed, displacement of LINC complexes from the nuclear envelope specifically eliminates perinuclear actin cap fibers, not basal or dorsal stress fibers 18 (results shown below). On the basis of these observations actin cap fibers are not considered part of the cortical actin network in contact with the plasma membrane, but rather are uniquely connected to the nucleus.

Herein we now show that actin cap associated focal adhesions are fundamentally distinct from basal or dorsal actin filament associated conventional focal adhesions in their morphology, size, spatial distribution, movement, turnover dynamics, topological connections to actin filament in the cell, and importantly response to mechanical cues. In particular, our results indicate that actin cap associated focal adhesions that are under higher tension due to the connection to the actin cap fibers are more sensitive to changes in substrate compliance than conventional focal adhesions. This early differential response of actin cap associated focal adhesions compared to conventional focal adhesions is mediated by myosin II in combination with the actin crosslinking protein α-actinin in actin cap fibers, the attachment of actin cap fibers through LINC connections to the nucleus, and the activity of focal adhesion kinase (FAK) in actin cap associated focal adhesions, but not focal adhesion proteins paxillin, talin, and zyxin.

Results

Actin cap associated focal adhesions have distinct morphology, dynamics, and spatial distribution. By lowering the plane of focus of a fluorescence microscope, the highly ordered actin cap fibers that drape over the top of the interphase nucleus of mouse embryonic fibroblasts (Fig. 1, A–C) were progressively followed along their length, from the top of the nucleus to their terminations at the basal surface (Fig. 1D and Suppl. Movie 1). This procedure revealed the existence of vinculin-containing focal adhesions at the ends of the individual actin cap fibers (red structures in Fig. 1, C and D). Focusing on the basal cellular layer also showed the presence of conventional focal adhesions terminating conventional basal actin fibers (yellow structures in Fig. 1, C and D),

We asked whether this topologically defined subset of focal adhesions (connected to the perinuclear actin cap fibers) was morphologically and functionally different from conventional focal adhesions. The number of stress fibers on top of the nucleus was much smaller than the number of conventional stress fibers at the basal surface of cells; accordingly the number of actin cap associated focal adhesions terminating these stress fibers was less than the number of conventional focal adhesions, representing only ~30% of all focal adhesions per cell (Fig. 1, E and F). Actin cap associated focal adhesions were longer than conventional focal adhesions and thus they showed significantly larger area (Fig. 1, G and H) as well as a more elongated shape, corresponding to a lower shape factor (Fig. 1I), defined as $4\pi A/P^2$ (where A and P are area and perimeter of a focal adhesion, approaching 1 for a rounded and 0 for an elongated focal adhesion).

Unlike conventional focal adhesions, which were dispersed throughout the cellular basal surface, actin cap associated focal adhesions were almost exclusively located at the cell periphery (Fig. 1J, where relative position is defined as D/R where D is the distance between geometric centers of the cell and focal adhesions and R is the effective radius of the cell calculated by $\sqrt{\text{Cell area}/\pi}$ so 1 corresponds to a position at the periphery, 0 a position at the center of the cell), within the two narrow sectors situated in the direction of the parallel actin cap, which coincided with the overall orientation of the cell and the long axis of the nucleus (e.g. Fig. 1, C and D). Hence despite the fact that actin cap fibers are located on top of the nucleus, their associated focal adhesions are distal from the nucleus. Live-cell movies showed that actin cap associated focal adhesions maintained this peripheral location over long observation times (Suppl. Movie 2). Together, these results indicate that actin cap associated focal

adhesions have significantly different morphology and spatial distribution in the cell from those of conventional focal adhesions.

Latrunculin B treatment of cells revealed that actin cap fibers underwent much faster disassembly than basal stress fibers during the same treatment time (Fig. 2, A, B, D, E, G, and H). Accordingly the number of actin cap associated focal adhesions decreased more significantly than conventional focal adhesions (Fig. 2, C, F, and I). Since latrunculin B sequesters actin monomers away from the polymerizable actin pool so that abolishes stress fiber formation these results indicate that actin cap fibers are more dynamic than basal stress fibers, suggesting another difference between actin cap associated focal adhesions and conventional focal adhesions.

Because actin cap fibers are more dynamic than basal stress fibers, we hypothesized that turnover in the actin cap associated focal adhesions was faster than in the conventional focal adhesions. To assess the turnover dynamics of focal adhesions, cells were doubly transfected with EGFP-paxillin and RUBY-Lifeact (Fig. 3A and Suppl. Movie 2). Actin cap associated focal adhesions and conventional focal adhesions were distinguished in live cells following the procedure described in Fig. 1D. Fluorescence recovery after photobleaching (FRAP) analysis of paxillin-EGFP for the two types of focal adhesions selected from the same cell showed that actin cap associated focal adhesions had a significantly shorter half-time of recovery than conventional focal adhesions (Fig. 3C). Comparison of recovery half-time in the tested cells also showed that fluorescence in actin cap associated focal adhesions was always recovered systematically faster than conventional focal adhesions (Fig. 3D).

Following Burnette et al.[24] using time-lapsed confocal imaging of the same doubly transfected cells, we also measured the displacements of focal adhesions by tracking the positions of their centroids[25,26]. We found that the averaged speed of the movements of actin cap associated focal adhesions was significantly higher than the speed of conventional focal adhesions (Fig. 3, A and B, and Suppl. Movie 2). These results suggest that actin cap associated focal adhesions are larger but more dynamic than conventional focal adhesions, potentially facilitating a more rapid response to extracellular stimuli (see more below).

Together these results identify actin cap associated focal adhesions differ from conventional focal adhesions in morphology, size, spatial distribution in the cell, turnover dynamics, and speed.

Synergistic regulation of actin cap fibers and associated focal adhesions by myosin II and α-actinin. Given the larger size (i.e. area) and elongated shape of individual actin cap associated focal adhesions, since size and shape of focal adhesions depend on tension[27], we asked whether there was any difference in the degree of contractility required for formation of actin cap associated focal adhesions compared to conventional focal adhesions. The response of conventional and actin cap associated focal adhesions was examined in cells treated with varying concentrations of the myosin light chain kinase (MLCK) inhibitor ML-7 (Fig. 4, A–L). At 10 μM concentration of ML-7, cells continued to show normally organized basal actomyosin filament bundles (Fig. 4J) that contained phospho-myosin light chain 2 (p-MLC2) (Fig. 4 K and L), little changed from basal stress fibers in control untreated cells (Fig. 4, D–F). Accordingly, conventional focal adhesions in ML-7 treated cells were unchanged in number (Fig. 4M), size (Fig. 4N), and shape (Fig. 4O). In contrast, at this low concentration of ML-7, the actomyosin bundles in the perinuclear actin cap showed disorganized p-MLC2 staining (Figs. 4 H *vs.* 4B) and the size and shape of actin cap associated focal adhesions were significantly affected (Fig. 4, C, I, N, and O) while F-actin structure was not disrupted (Figs. 4 G *vs.* 4A) and thus the number of actin cap associated focal adhesions was unchanged (Fig. 4M). These results suggest that phospho-myosin-mediated tension in actin filaments is not required for the maintenance of the perinuclear actin cap fibers
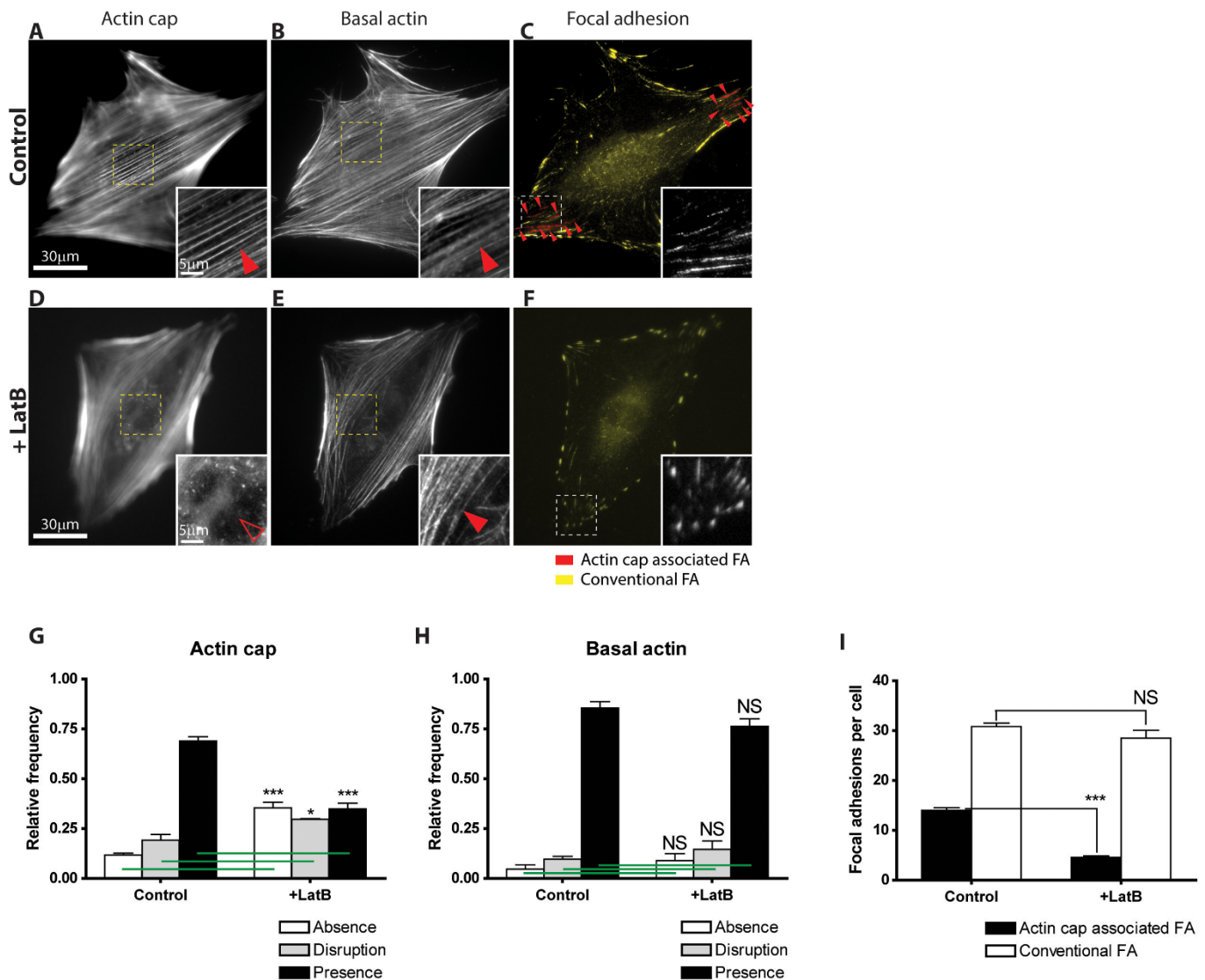
Figure 2 | **Differential response of actin cap and actin cap associated focal adhesions to inhibition of actin assembly.** (A–F) Actin filament organization on top of the nucleus (A and D) and at the cellular basal surface (B and E) and typical morphology of actin cap associated focal adhesions (red, arrowheads) and conventional focal adhesions (yellow) in those cells (C and F) on collagen I-coated glass substrates, in the absence (control, A–C) and the presence (+ latB, D–F) of a low dose of the actin-sequestering drug latrunculin B. Focal adhesions are marked by an antibody against vinculin and examined under fluorescence microscopy. Insets, details of actin cap. Full arrowheads point to well-organized perinuclear actin cap (A) and well-organized basal stress fibers (B and E), while open arrowheads point to absent perinuclear actin cap (D). (G) and (H) Proportion of control and latrunculin-B-treated cells showing a well-organized (black), disorganized (grey), or no (white) actin cap fibers (G) and well-organized (black), disorganized (grey), or no (white) basal stress fibers (H). Illustrative examples of these organizations of the actin cap and basal stress fibers are shown in the insets in panels A, B, D and E. (I) Number of actin cap associated focal adhesions (black bars) and conventional focal adhesions (white bars) per cell treated or not with latrunculin B. In panels G and H, at least 300 cells were analyzed for each condition and repeated 5 times in control and 3 times in latrunculin B treated cells; In panel I, 50 cells in control and 30 cells in latrunculin B treated condition were analyzed. ***: P < 0.001; *: P < 0.05; NS: P > 0.05.

but regulates the size and shape of actin cap associated focal adhesions.

Since 10 μM MLCK inhibition did not disassemble actin cap fibers (Fig. 4G), we asked whether F-actin crosslinking/bundling proteins played a distinguishing role in the maintenance or formation of actin cap fibers and associated focal adhesions relative to conventional fibers and their associated focal adhesions. We found that the depletion of the F-actin crosslinking/bundling protein α-actinin 1, 4 reduced the thickness of both basal and actin cap fibers and reduced the size of both corresponding focal adhesions (Fig. S1, A–F, and Insets). However, when α-actinin-depleted cells were treated with MLCK inhibitor ML-7, actin cap fibers were dismantled without significant change in basal stress fibers. Correspondingly, actin cap

associated focal adhesions were dissociated, but basal stress fiber associated conventional focal adhesions persisted (Fig. S1, G–I). These results suggest that F-actin binding protein α-actinin and phospho-myosin differentially regulate the actin cap and basal stress fibers and their associated focal adhesions.

Actin cap associated focal adhesions dominate early mechanosensing. Focal adhesions in adherent cells serve as a nidus for the mechanosensing of substrate compliance; they mediate the ability of a cell to sense and adapt to the mechanical properties of its microenvironment. We asked whether actin cap associated focal adhesions played a distinct role in mechanosensing by adherent cells. Cells were deposited on either stiff glass substrates - the
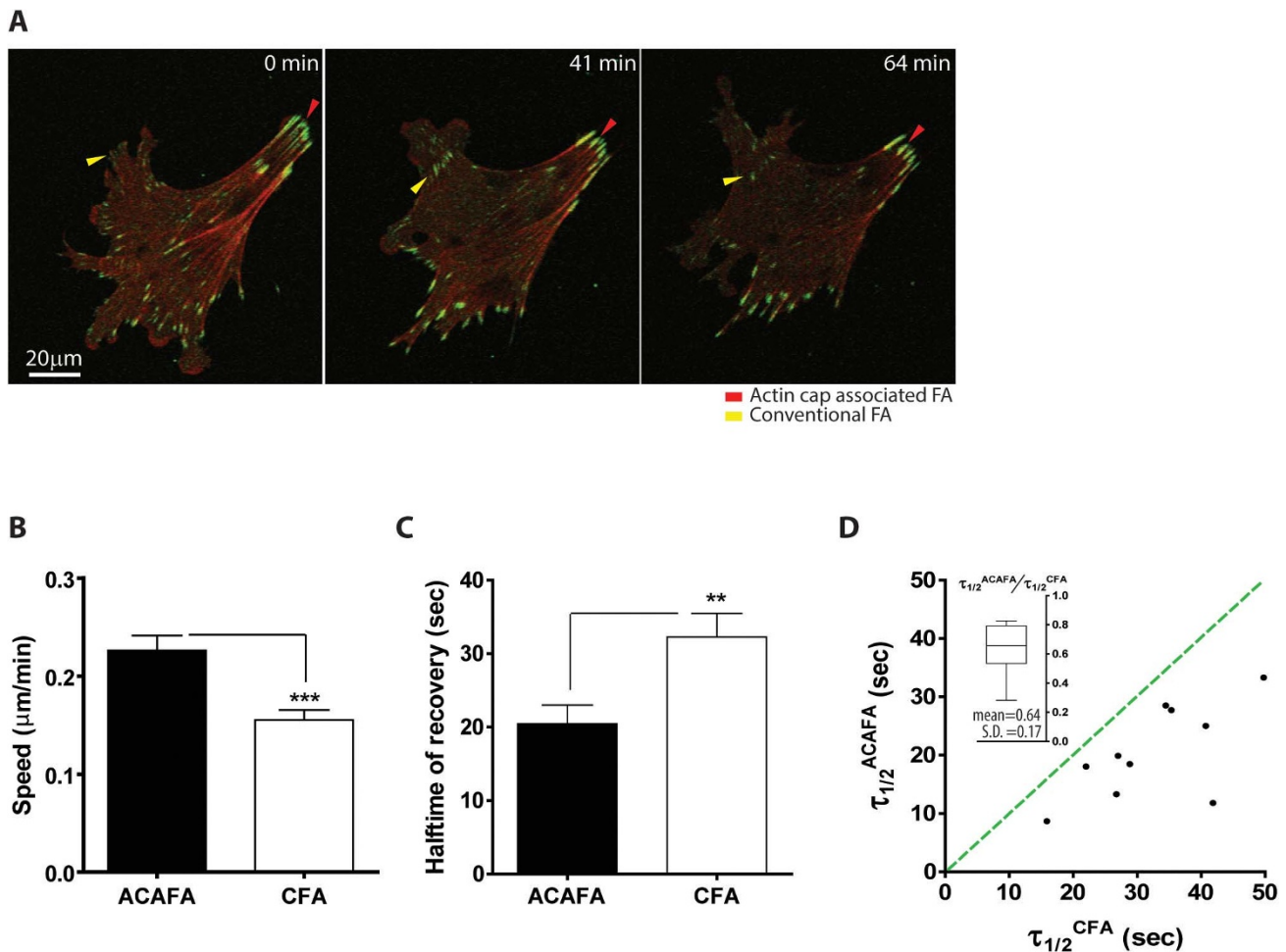
Figure 3 | Dynamics of actin cap associated focal adhesions and conventional focal adhesions. (A) Movements of an actin cap associated focal adhesion (red arrow) and a conventional focal adhesion (yellow arrow) in a cell transfected with RUBY-lifeact and EGFP-paxillin to simultaneously monitor actin and focal adhesion dynamics, respectively. The movie was captured by time-lapsed confocal microscopy. Conventional and actin cap associated focal adhesions were distinguished from one another by following actin cap fibers by lowering the plane of focus of the microscope (see method in Fig. 1D). (B) Averaged speed of actin cap associated focal adhesions (ACAFA) and conventional focal adhesions (CFA). Twenty focal adhesions of each type were analyzed. ***: P < 0.001. (C) Averaged half-time of fluorescence recovery of actin cap associated focal adhesions (ACAFA) and conventional focal adhesions (CFA) after photobleached in the outer half side. Each type of focal adhesion was identified in the same cell. 10 cells were analyzed. **: P<0.01. (D) Comparison of half-time of fluorescence recovery ($\tau_{1/2}$) of actin cap associated focal adhesions (ACAFA) and conventional focal adhesions (CFA). Slope of green dotted line is 1. *Inset*, relative fluorescence recovery. Note the values are always less than 1.

situation analyzed thus far - or soft polyacrylamide gels on glass. The elasticity of crosslinked polyacrylamide measured by AFM was significantly softer than glass (5 kPa and 500 kPa, respectively). Both glass and crosslinked polyacrylamide substrates were covered with the major extracellular matrix molecule collagen I so as to maintain the same biochemical presentation of extracellular-matrix ligands to the cells. We found that perinuclear actin cap fibers responded much more readily to changes in substrate compliance than conventional stress fibers at the basal surface of the cells (Fig. 5, A and B). The actin cap fibers were significantly disrupted and often disappeared altogether when cells were placed on soft substrates (Fig. 5A). Remarkably, the organization of conventional basal stress fibers was statistically unchanged over the same range of changes in substrate compliance (Fig. 5B).

Since cells on soft substrates showed disrupted actin cap fibers without disorganized basal actin fibers, we investigated whether actin cap associated focal adhesions also responded differently from conventional focal adhesions to changes in substrate compliance. The presence of actin cap associated focal adhesions was investigated not only by vinculin-staining (Figs. 5, C–F and S2, G–K) but also using antibodies against a variety of important focal adhesion proteins,

including paxillin, FAK, and zyxin (Fig. S2, A–H). Analysis of fluorescence micrographs (Figs. 5, C–D and S2, A–F) shows that number (Fig. S2G) and total area (Fig. S2H) of actin cap associated focal adhesions per cell area were significantly reduced in cells on soft substrates compared to cells on stiff substrates, and that the size (Fig. 5E) and length (Fig. S2I) of the remaining actin cap associated focal adhesions were also significantly reduced. In contrast, the size, number density (i.e., number per cell area), and area density (i.e., total area per cell area) of conventional focal adhesions remained statistically unchanged (Figs. 5, C–E and S2, A–H).

Following placement of cells on soft substrates, remaining actin cap associated focal adhesions were found more closely to the center of the cell (corresponding to 0 in relative position), while relative position of the conventional focal adhesions remained unchanged (Fig. 5F). Similarly, the speed of displacements of actin cap associated focal adhesions was reduced more than conventional focal adhesions (Fig. S2L). Together, these results indicate that actin cap associated focal adhesions respond to changes in substrate compliance much more readily than conventional focal adhesions (summarized in Fig. 5G).

As expected, all focal adhesions and stress fibers largely disappeared on extremely soft substrates (<1 kPa), indicating that
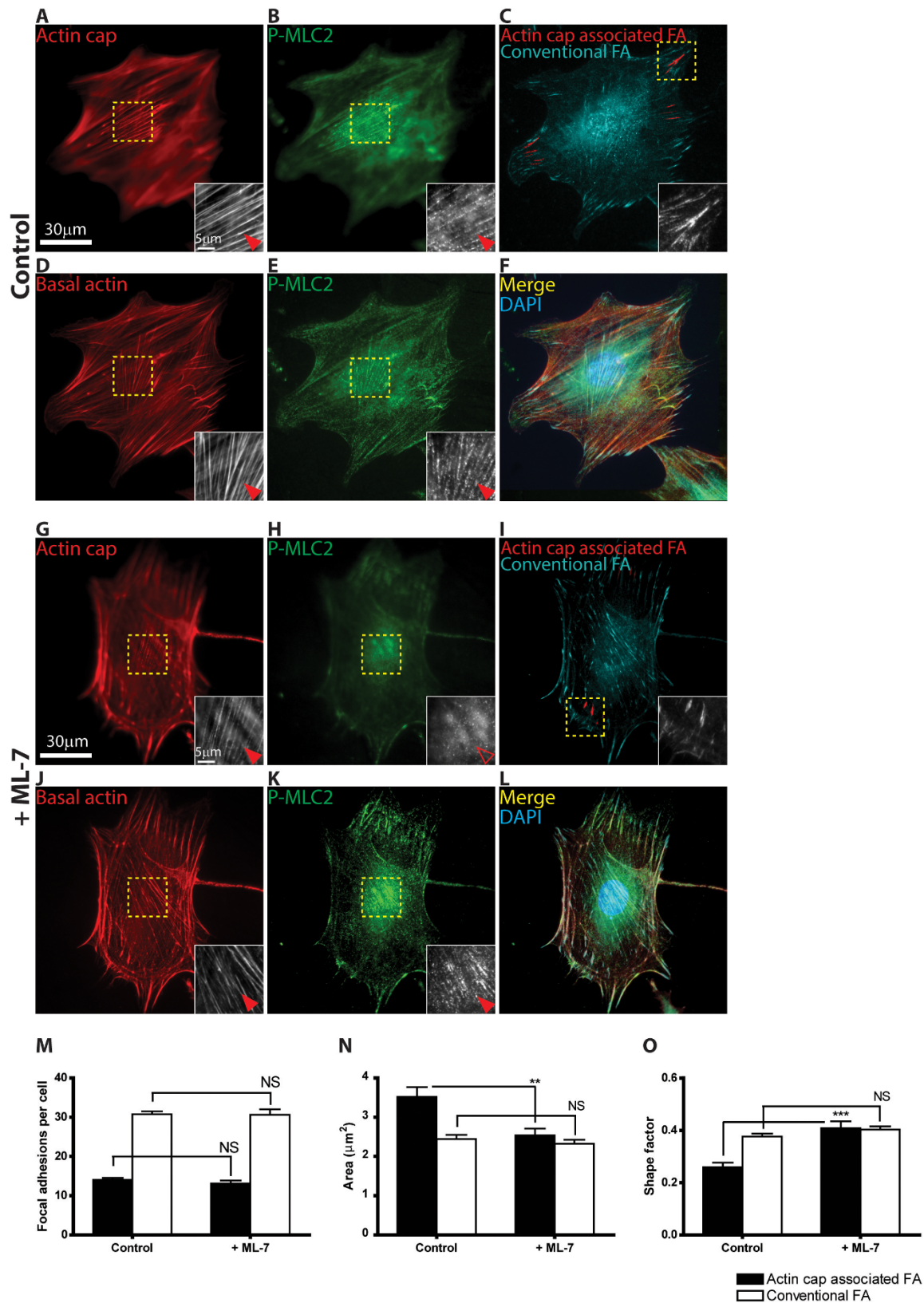
Figure 4 | Differential content in p-MLC2 and contractility of the perinuclear actin fibers. (A–L) Organization of actin filament (A, D, G, J) and p-MLC2 content (B, E, H, K) in the perinuclear actin cap (A, B, G, H) and basal stress fibers (D, E, J, K, and merged in F and L) in control cells (A–F) and cells treated with MLCK inhibitor ML-7 (G–L). Focal adhesions are marked by a vinculin antibody (C and I). *Insets* show details of F-actin organization, p-MLC2 content, and focal adhesion structure in the regions of interest shown in the panels. Full and open arrowheads point to well-organized fibers and absence of well-organized fibers at the top of the nucleus (A, G) or the basal cell surface (D, J), respectively, or high and low p-MLC2 content in actin fibers (B, E, H, K), respectively. (M–O) Number per cell (M), average area (N), and shape factor (O) of actin cap associated focal adhesions (black bars) and conventional focal adhesions (white bars) in control and ML-7 treated cells. For each condition in panels M–O, 50 cells in control and 30 cells in ML-7 treated cells were examined (M) and at least 300 focal adhesions were analyzed for each condition (N and O). ***: $P < 0.001$; **: $P < 0.01$; NS: $P > 0.05$.
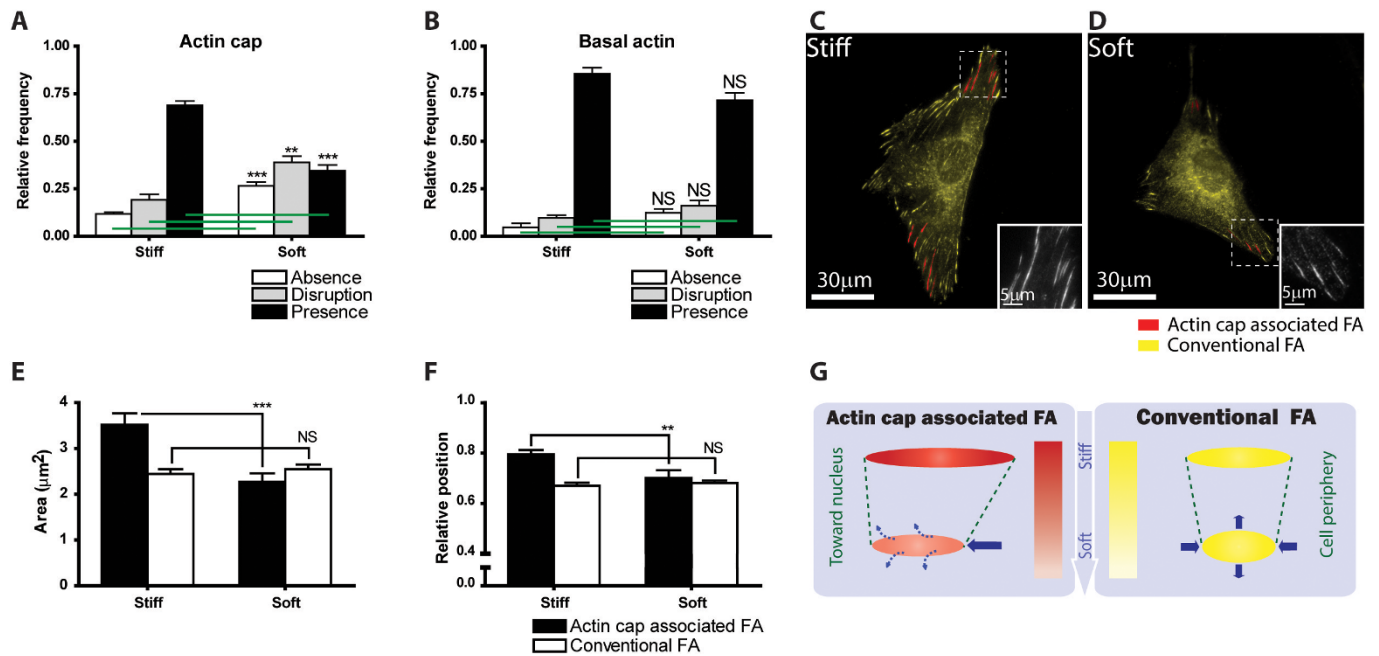
Figure 5 | Differential response of actin cap and actin cap associated focal adhesions to changes in substrate compliance. (A) and (B) Proportion of cells showing a well-organized (black), disorganized (grey), or no (white) actin cap (A) and basal actin stress fibers (B) on stiff and soft substrates. (C) and (D) Representative organization and number of actin cap associated focal adhesions (red) and conventional focal adhesions (yellow) in WT cells placed on stiff (C) and soft substrate (D). *Insets*, details of (unlabeled) focal adhesions in control cell. (E) and (F) Changes in average surface area (E) and relative position between the periphery (1) and the center (0) of the cell (F) of actin cap associated focal adhesions (black bars) and conventional focal adhesions (white bars) in response to changes in substrate compliance. (G) Schematic of the differential regulation of size, shape, length, breadth, and position of actin cap associated focal adhesions and conventional focal adhesions by substrate compliance (also based on data in Fig. S2, S4, and S5). In panels A and B, at least 300 cells were analyzed for each condition and repeated 5 times in WT control and 3 times in the other conditions; In panels E and F, at least 300 focal adhesions were analyzed for each condition; ***: $P < 0.001$; **: $P < 0.01$; NS: $P > 0.05$.

conventional focal adhesions also participate in the mechanosensing response, but that a much larger amplitude of mechanical stimulus is required (Fig. S3). Together these results suggest that early sensing of the compliance of the matrix environment by adherent cells is dominated by the small subset of large focal adhesions that physically connect the underlying substratum to the actin cap stress fibers.

Mechanosensing by actin cap associated focal adhesions is uniquely mediated by FAK. We noted that pFAK [Y397] staining within individual actin cap associated focal adhesions, when normalized by total FAK staining, was significantly higher than in conventional focal adhesions on stiff substrate (Fig. S4A), but this difference was eliminated in cells on soft substrates where most of actin cap fibers and associated focal adhesions were disrupted (Fig. S4B). This result revealed that FAK was more activated in the actin cap associated focal adhesions than in conventional focal adhesions on stiff substrates. This prompted us to ask the following two questions: First, are actin cap associated focal adhesions more sensitive to the force applied to them than conventional focal adhesions? Second, do FAK and/or other focal adhesion proteins mediate the distinct response of actin cap associated focal adhesions to changes in substrate compliance?

To address the first question, we quantitatively analyzed immunomicrographs of vinculin using constant camera settings and found that vinculin content was significantly higher in actin cap associated focal adhesions than in conventional focal adhesions (Fig. S5). This result and the previous analysis on pFAK content suggest that actin cap associated focal adhesions are under higher tension than conventional focal adhesions since FAK activation and vinculin recruitment require myosin II dependent tension[28]. These results suggest that actin cap associated focal adhesions are under high tension which in turn induces actin cap associated focal adhesions to be

significantly larger and more elongated than conventional focal adhesions[27]. A recent model by Walcott and Sun[29] shows that size of focal adhesions alone is a major determinant of mechanosensitivity (see more under Discussion).

FAK, talin, and zyxin have all been proposed as mediators of mechanosensing[5,16,27,30–32]. To determine whether the major focal adhesion-specific enzyme FAK was involved in the mechanosensory response of actin cap associated focal adhesions, we RNAi-depleted FAK from cells (Fig. S6) and determined the response of both actin cap and basal actin stress fibers and associated focal adhesions to changes in substrate compliance. The change in the number of actin cap associated focal adhesions (normalized by the total number of focal adhesions) was mostly abrogated in FAK-depleted cells compared to control WT cells (Fig. 6, B, E, and H). We also found that the fraction of FAK-depleted cells featuring actin cap fibers on soft substrates was higher than in control cells and they kept normal organization of basal stress fibers (Fig. 6, A, C, D, F, and G). Hence, the presence of FAK in adherent cells mediates the ability of their actin cap associated focal adhesions to sense and respond to changes in substrate compliance.

In contrast, the depletion of the focal adhesion protein zyxin had no significant effect on the response of actin cap associated focal adhesions to changes in substrate compliance compared to control cells (Fig. 6B). The organization of actin cap fibers (Fig. 6A) and the number of actin cap associated focal adhesions (Fig. 6B) in zyxin-depleted cells on soft substrates diminished similarly to these structures in control cells. The same occurred for cells RNAi-depleted of paxillin and talin (Fig. 6, A and B). Hence, zyxin, paxillin, and talin did not influence the response of the actin cap and associated focal adhesions to changes in substrate compliance.

Together, these results suggest that the mechanosensory response of adherent cells is dominated by perinuclear actin cap fibers

7
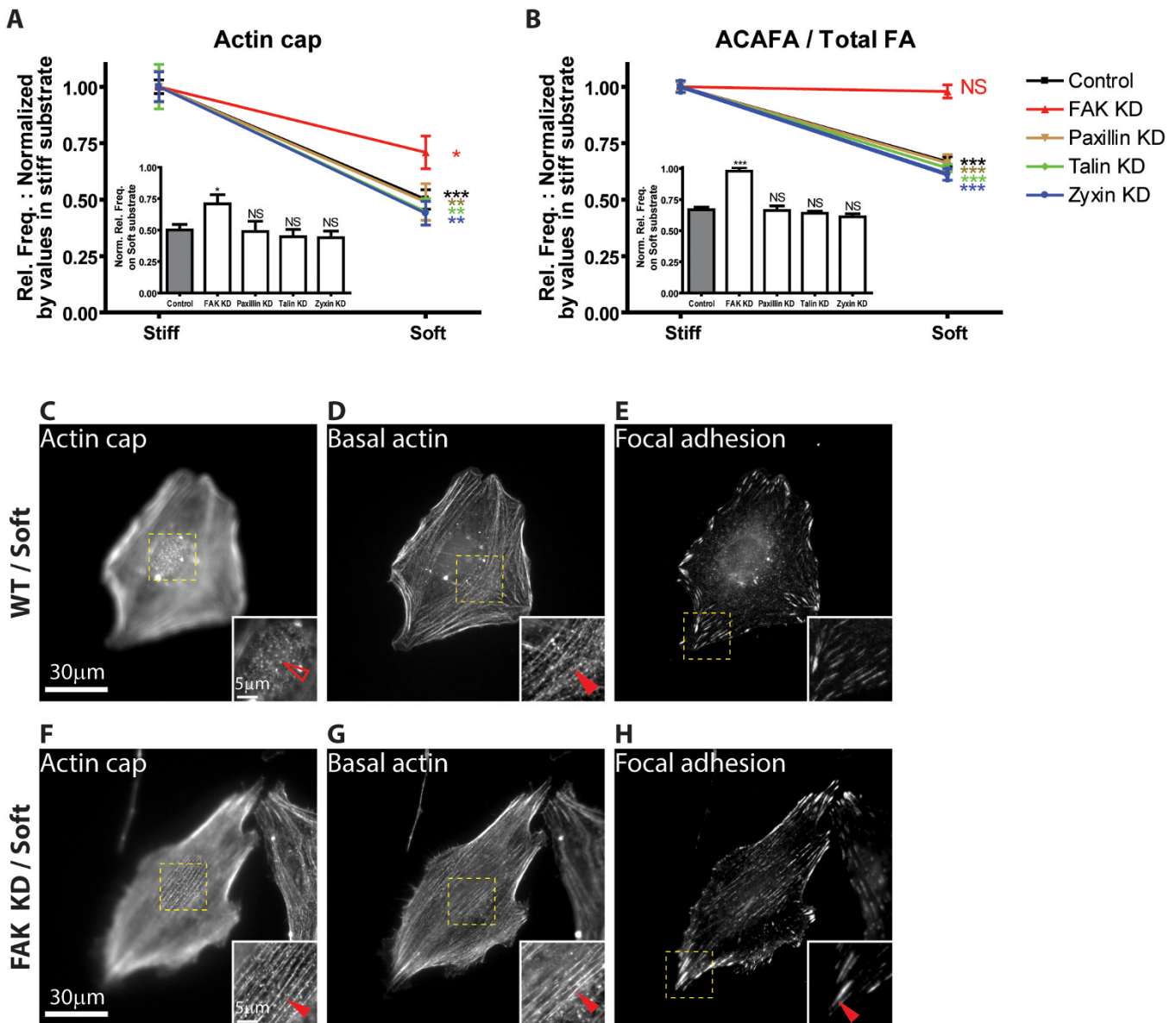
Figure 6 | Regulation of mechanosensing by actin cap associated focal adhesions through FAK. (A) and (B) Relative changes in the fractions of cells showing an organized perinuclear actin cap (A) and number of actin cap associated focal adhesions divided by the total number of focal adhesions (B) normalized by corresponding values on stiff substrates (i.e. on stiff, the value is always 1), for control WT cells, cells depleted of FAK, paxillin, talin, and zyxin on stiff and soft substrates. (C–H) Actin cap fibers (C, F), basal stress fibers (D, G), and vinculin-stained focal adhesions (E, H) in a WT cell (C–E) and a FAK-depleted cell (F–H) on soft substrates. This figure illustrates the lack of response of actin cap associated focal adhesions in FAK-depleted cells compared to control cells. *Insets.* Details of F-actin organization and focal adhesion structure. Full arrowheads point to well-organized actin stress fibers (D, F, G) or a specific actin cap associated focal adhesion (H) and open arrowhead point fully disrupted actin structure (C), respectively. In panel A, at least 300 cells were tested for each condition and repeated 5 times in WT control and 3 times in the other conditions; In panel B, 50 cells in control and 30 cells in the other conditions were analyzed; ***: P < 0.001; *: P< 0.05; NS: P > 0.05. One-way ANOVA analysis was applied to the bar graphs (Dunnett's multiple comparison test).

terminating focal adhesions where more tension applied than in conventional focal adhesions. Furthermore, actin cap associated focal adhesions are particularly more sensitive to FAK activity than conventional focal adhesions and mechanosensing by actin cap associated focal adhesions is mediated by focal adhesion-specific enzyme FAK, not by focal adhesion proteins zyxin, paxillin, and talin.

Formation and mechanosensing of actin cap associated focal adhesions is mediated by LINC complexes. Since LINC complexes anchor perinuclear actin cap fibers to the apical surface of the nuclear envelope[18], we asked whether displacing LINC

complexes from the nuclear envelope would affect the formation of actin cap associated focal adhesions and their ability to sense changes in substrate compliance. Cells were transfected with the well-characterized EGFP-KASH2 construct that displaces LINC complex proteins Nesprin2giant and Nesprin 3 from the nuclear envelope[33,34]. EGFP-KASH2-transfected cells on stiff substrates showed partially or totally disrupted actin cap structure and dramatic decrease in the number of large actin cap associated focal adhesions (Fig. 7 A–E), while cells transfected with the control construct EGFP-KASH2-ext showed no significant change in actin cap and basal stress fibers and their associated focal adhesions (Fig. 7, A–C, F, and G). Moreover, the few remaining actin cap associated
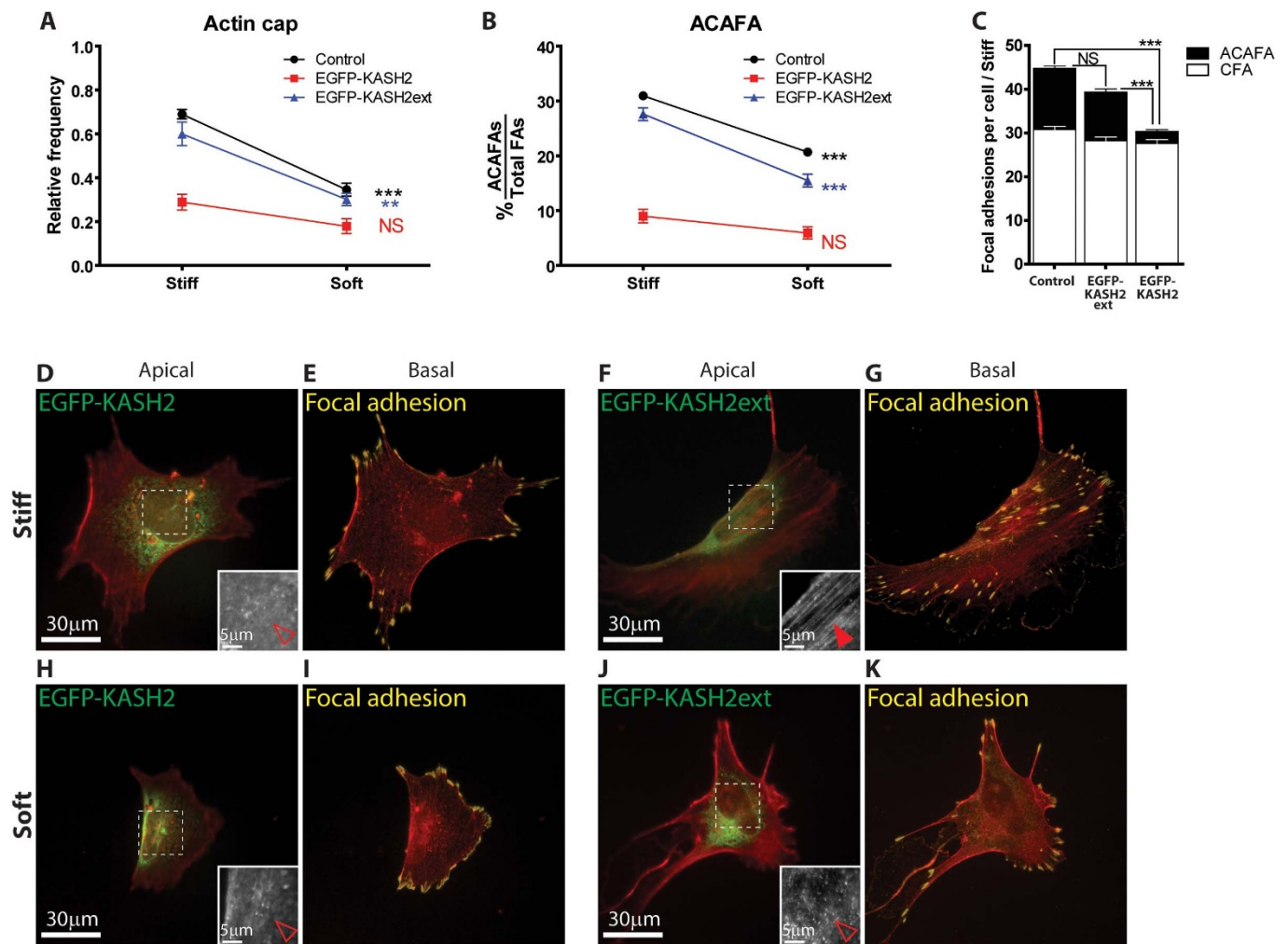
Figure 7 | The role of LINC complexes in actin-cap-mediated cellular mechanosensing. (A–C) Changes in the fraction of cells featuring an organized actin cap (A) and fraction of actin cap associated focal adhesions (B) in different substrates, total number of focal adhesions on stiff substrates (C) for control WT, cells transfected with control construct EGFP-KASH2ext, or EGFP-KASH2. 50 cells in control and 30 cells in each transfected condition were analyzed. ***: P < 0.001; **: P< 0.01; NS: P > 0.05. (D–K) F-actin organization (red) merged with EGFP-KASH2 or EGFP-KASH2ext constructs (green, D,F,H,J) and merged with vinculin stained focal adhesions (yellow, E, G, I, K) in the apical plane (F, D, H, J) and the basal plane (E, G, I, K) on stiff (D–G) and soft (H–K) substrate. *Insets,* details of F-actin organization. Full arrowheads point to well-organized perinuclear actin cap (F), while open arrowheads point to absence of actin cap fibers or basal stress fibers (D, H, and J).

focal adhesions in EGFP-KASH2-transfected cells were not nearly as responsive to changes in the substrate stiffness (Fig. 7, B, H–K). These results suggest that the formation and mechanosensing response of actin cap associated focal adhesions require the connections between the actin cap fibers and the nuclear envelope by LINC complexes (see schematic, Fig. 8A).
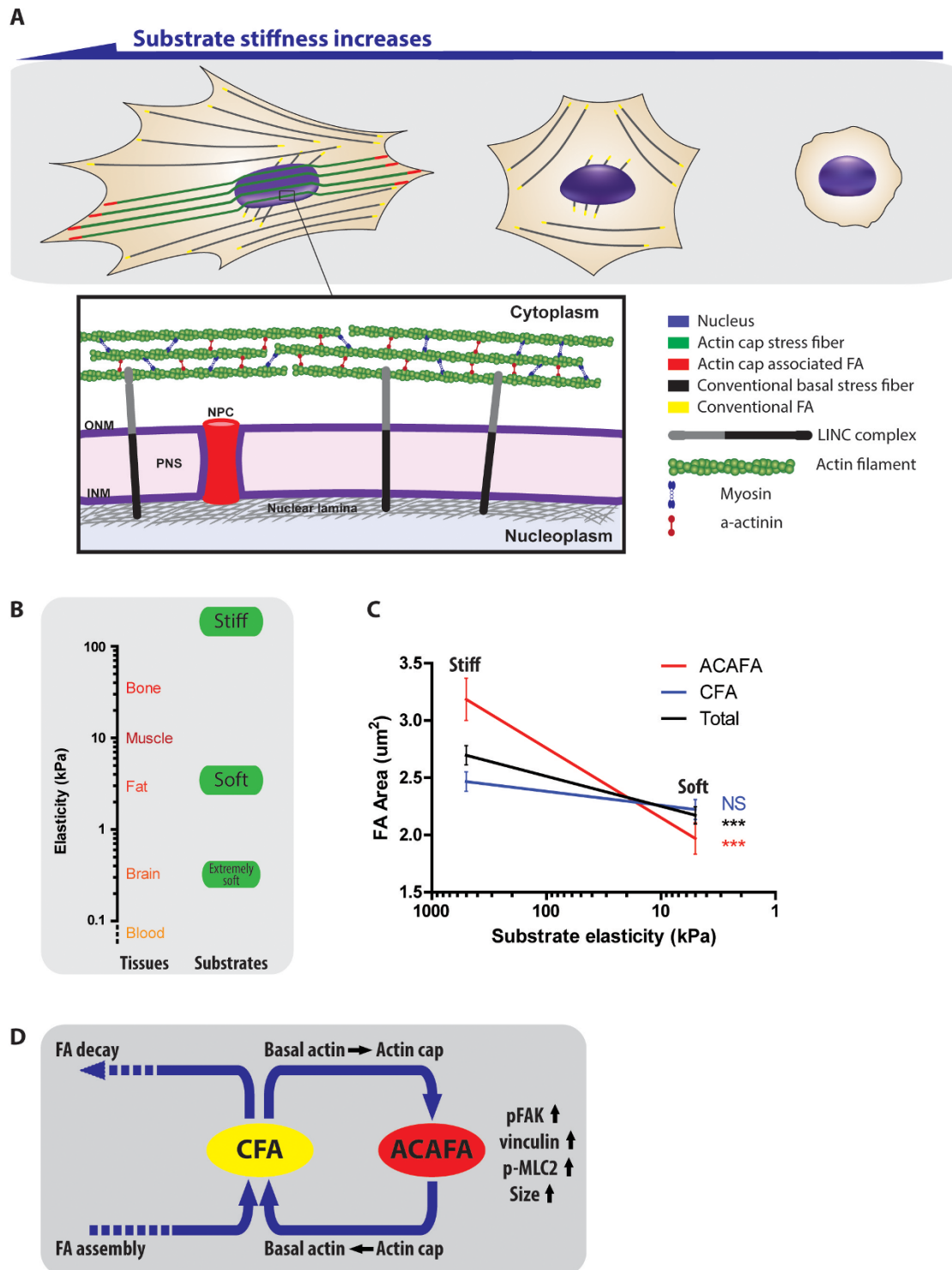
Mechanosensing by actin cap associated focal adhesions in human cells. Finally, we asked whether actin cap associated focal adhesions were present in human cells and also dominated their early mechanosensing response. Both human foreskin fibroblasts (HFFs) and human umbilical vein endothelial cells (HUVECs) featured prominent perinuclear actin cap fibers, on top of the interphase nucleus, and associated focal adhesions, which were similarly distributed at the edge of cell in the overall direction of the parallel actin cap stress fibers (Fig. S8, A–C and G–I). In these primary human cells, as in mouse embryonic fibroblasts, only actin cap fibers, not basal stress fibers, became disorganized or disappeared when cells were placed on soft substrates (Fig. S8, D, E, J, K). Accordingly, only actin cap associated focal adhesions, not conventional focal adhesions, responded to small changes in substrate compliance (Fig. S8, C, F, I, L).

One would predict that cells that do not display actin cap fibers would be less sensitive to substrate compliance changes. To test this prediction, we examined human osteosarcoma cells (U2OS), which did not feature an actin cap and associated focal adhesions, but showed arcs and dorsal stress fibers (Fig. S8, M–R). In agreement with our hypothesis of dominance of mechanosensing by actin cap associated focal adhesions, the basal and dorsal actin organization of U2OS cells placed on soft substrates were maintained and associated focal adhesions remained similar (Fig. S8, M–R).

These results suggest that the actin cap fibers and associated focal adhesions are present in human cells, and further establish these structures as functionally and structurally distinct from basal stress fibers and conventional focal adhesions that terminate them, in that they dominate early cellular mechanosensing.

Discussion
We have identified a distinct subset of focal adhesions, actin cap associated focal adhesions, which are different from conventional focal adhesions in size, shape, movement, turnover kinetics, cellular organization, and mechanosensing response to substrate compliance.

Figure 8 | The unique response of actin cap and actin cap associated focal adhesions in response to substrate compliance. (A) Schematic of the cellular mechanosensing in response to substrate compliance. Well-organized actin cap fibers (green) on top of the nucleus are terminated by ACAFAs (red) at the pheriphery of the adherent cell and nucleus (blue) is elongated in the same direction as actin cap fibers (Left). As substrate compliance increases, ACAFAs and actin cap fibers disappear, but CFAs (yellow) and basal actin fibers (black) remain and the nucleus becomes rounded (Middle). On extremely soft substrates, most actin stress fibers and focal adhesions disassemble and the nucleus is more rounded (Right). *Inset.* Physical connections between actin cap stress fibers and nucleus through the linker of nucleoskeleton and cytoskeleton (LINC) complexes. PNS: perinuclear space; INM: inner nuclear membrane; ONM: outer nuclear membrane. By disrupting LINC complexes, actin cap fibers become disorganized and mechanosensing controlled by actin cap associated focal adhesions is suppressed. (B) and (C) The extremely wide range of substrate stiffness for which only ACAFAs respond (B). Tissue elasticity data adapted from Buxboim *et al.*[38]. Response of the size of focal adhesions to substrate stiffness changes (C). Data adapted from Figure 5E was replotted. ***: P < 0.001; NS: P > 0.05. (D) Schematic of the conversion of ACAFAs from CFAs. Dynamic movements of the nucleus induce conventional focal adhesions to turn into actin cap associated focal adhesions, which is accompanied by increases in pFAK, vinculin, and p-MLC2 contents and an increase in the size of focal adhesions. *Vice versa*, actin cap associated focal adhesions can turn into conventional focal adhesions as actin cap fibers turn into basal stress (see also Fig. S10 and Suppl. movie 3).

Over an extremely wide range of substrate stiffness (from stiffness of glass (≫100 kPa) to that of adipose tissue (~5 kPa)), corresponding to most tissues, only actin cap fibers and actin cap associated focal adhesions respond to stiffness changes (Fig. 8 A and B). Well-characterized conventional focal adhesions only respond when cells are exposed to the stiffness corresponding to soft brain tissue (<1 kPa). When not distinguishing these two types of focal adhesions, one would observe global changes in focal adhesions. But now that we have defined and characterized actin cap associated focal adhesions, we know that this global response is largely dominated by actin cap associated focal adhesions (Fig. 8C).

Why are actin cap associated focal adhesions more responsive to changes in substrate compliance than conventional focal adhesions? A recent computational model by Walcott and Sun[29] shows that, regardless of molecular composition, large focal adhesions (such as actin cap associated focal adhesions) will respond more readily to changes in environmental tension, than small focal adhesions (such as conventional focal adhesions) (Fig. S9). According to this model, a relatively small difference in focal adhesion size (30%) can indeed lead to a large change in the probability of focal adhesion formation, in agreement with our experiments (Figs. 1G and 5E). Our results suggest the mechanism that renders actin cap associated focal adhesions larger than conventional focal adhesions: actin cap fibers are under more tension, presumably caused by the pressure exercised by the nucleus and more tension is known to generate larger focal adhesions[27]. This mechanism is supported by the significantly higher vinculin content in actin cap associated focal adhesions (Fig. S5), as vinculin content correlates with enhanced fiber tension[35]. Hence an increase in the concentration of mechanosensing protein vinculin will increase the ability of actin cap associated focal adhesions to sense substrate stiffness compared to conventional focal adhesions. The higher sensitivity of actin cap fibers to inhibition of myosin II contractility further implies that they are under increased tension compared to basal stress fibers. Inhibition of phosphorylation of myosin II by ML-7 treatment affects mostly p-MLC2 content in the actin cap fibers, not basal actin fibers (Fig. 4), and ML-7 abrogates the response of actin cap fibers and associated focal adhesions to changes in substrate compliance. Hence Walcott and Sun's model, whose simple underlying assumptions are verified by our experimental results, suggests that the much greater response of actin cap associated focal adhesions to substrate compliance is due to their larger size, which is caused by higher tension in the actin cap fibers.

Mechanosensing by actin cap associated focal adhesions is uniquely regulated by FAK (Fig. 6 and Fig. S7). To confirm the role of FAK in actin cap associated focal adhesion-specific mechanosensing, we reintroduced EGFP-FAK-wt or EGFP-FAK-Y397F to the FAK-depleted cells. The mechanosensing response of FAK-depleted cells rescued in both cases (Fig. S7, A–J). Interestingly, autophosphorylation-defective FAK mutation (FAK-Y397F) could also rescue cell mechanosensing to the same extent as control cells (Fig. S7 A, B, and K–R). These results imply that phosphorylation in Y397 is important for the optimal function of FAK, but it is not always necessary in mechanosensing by adherent cells. We think that FAK activity is still somewhat active (even weak) in FAK-Y397F and actin cap associated focal adhesions are extremely sensitive to the FAK activity and thus even in this weak level of activity in the Y397F they are able to sense the changes in the substrate stiffness.

Conventional and actin cap associated focal adhesions share many molecular components. This may have hindered the identification of actin cap associated focal adhesions as a molecularly and functionally distinct subset of focal adhesions. An explanation for these similar molecular compositions for both types of adhesions is provided by time-lapse confocal movies of cells showing focal adhesions dynamics as well as nuclear movements (Suppl. Movie 2). Indeed, a subset of focal adhesions that terminate actin cap fibers will remain actin cap associated focal adhesions until the contractile actin cap fibers move the nucleus while sliding along the side of the nucleus towards the basal cell surface (See also Suppl. Movie 3 and Fig. S10). As actin cap fibers squeeze the nucleus, the nucleus can escape the cage formed by actin cap fibers and move away from them, which subsequently turns these fibers into basal stress fibers. Vice versa, the nucleus can reposition itself underneath nearby basal stress fibers, which can turn these basal stress fibers into new actin cap fibers. As a result, due to the nuclear movements, actin cap fibers can switch into conventional basal fibers and the corresponding actin cap associated focal adhesions can become conventional focal adhesions and *vice versa* (Fig. 8D).

This work suggests the existence of a topologically connected physical pathway mediating mechanosensing by adherent cells. This long-speculated physical pathway directly links the compliant substratum to the cell through a small subset of focal adhesions - the actin cap associated focal adhesions, which are connected to a small subset of actin filaments, the actin cap fibers, which are connected to the nuclear envelope through the LINC complexes[18], which themselves interact directly and indirectly to chromosomal DNA through lamin A/C and accessory proteins. These findings raise the possibility that the actin cap associated physical pathway(s) may regulate gene expression and/or DNA replication. Future work will determine whether the actin cap fibers and actin cap associated focal adhesions play an important role in durotaxis[30] and the directed differentiation of stem cells[4,36] by substrate compliance, two processes that require mechanosensing.

Methods

Cell culture. Mouse embryonic fibroblasts (MEFs) and human foreskin fibroblasts (HFFs) were cultured in Dulbecco's Modified Eagle's Medium (DMEM, ATCC, Manassas, VA) supplemented with 10% fetal bovine serum (FBS, ATCC), 100 U/ml penicillin, and 100 μg/ml streptomycin (Sigma, St. Louis, MO). MEFs infected with shRNA constructs were initially selected with 4μg/ml puromycin (Sigma) containing medium for three days and then maintained in 3μg/ml puromycin added medium. Human osteosarcoma cells (U2OS) were cultured in McCoy's 5A medium (Gibco, Carlsbad, CA) supplemented with 10% fetal bovine serum (FBS, ATCC), 100 U/ml penicillin, and 100μg/ml streptomycin (Sigma, St. Louis, MO). Human umbilical vein endothelial cells (HUVECs) were grown in HUVEC's complete growth medium which is Ham's F-12 Kaighn's modification (F-12K, ATCC) supplemented with 0.1 mg/ml of heparin (Sigma), 0.05 mg/ml of endothelial cell growth supplement (ECGS, Sigma), and 10% fetal bovine serum (FBS, ATCC). Cells were maintained at 37°C with 5% CO_2 in a humidified incubator and passaged every 3–4 days.

Protein depletion. Three or four RNAi sequences targeting mRNA of each studied molecule were selected as described[37]. After testing in MEFs with lentiviral mediated RNAi, we selected those that showed more than 90% knocking down efficiency for subsequent experiments. They include (the number after the sequence denotes the targeting position in mRNA): mh-Talin1,2GTGGATGAGAAGACCAAGGA (1372); mh-Talin1,2 GCCAAGGTGATGGTGACCAA (6706); mh-Paxillin gCCTGGATAAAGTGGTGACA (1325); mh-Paxillin gTCAAGGAGCAGAACGACAA (1770); mh-FAK GGGCATCATTCAGAAGATA (507); mhFAK GGATTTCTAAACCAGTTTA (661); m-ACTN1,4 GGAGGACTTCCGAGACTATA (1164); mh-ACTN1,4 GCAGAGAAGTTCCGGCAGA (1299); m-Zyxin GCCTGTGTCTTCTGCTAATA (1004); m-Zyxin GGACAACTGTTCCACATCA (1484); A firefly luciferase shRNA was used as a control (5′- GCTTACGCTGAGTACTTCGA). Using the predicted sequences above, the shRNA expression cassettes were constructed by joint PCR, as described[37].

Drug treatment and cell transfection. F-actin depolymerising drug latrunculin B (Sigma), MLCK inhibitor ML-7 (Sigma), and myosin II inhibitor blebbistatin (Sigma) were diluted to final concentrations of 60 nM, 10 μM, and 15 μM, respectively, by using the stock solutions. Cells were incubated with each drug added culture medium for 1 hour. The transfection complex was prepared in Opti-MEM I reduced serum medium (Gibco, Carlsbad, CA) and FuGENE HD (Roche, Indianapolis, IN) was used as a transfection agent. The amount of DNA loaded and mixing ratio were determined following the supplier's suggested instructions.

Substrate preparation. Soft substrates were prepared by synthesizing polyacrylamide gel (PAG) onto the 3-aminopropyltrimethoxysilane and 10% of glutaraldehyde treated glass slides by using established methods[2]. Acrylamide and

N,N-methylenebisacrylamide were mixed at a final concentration of 5% and 0.15% (for soft substrate or 0.015% for extremely soft substrate) in distilled H_2O (w/v), respectively. To initiate free radical polymerization, 10% ammonium persulfate and N,N,Ń,Ń-tetramethylethylenediamine (TEMED, Invitrogen) were introduced as 5% and 0.5% (v/v) of total mixture. During polymerization, dichlorodimethylsilane treated nonreactive glass coverslip was overlaid onto the solution droplet to prepare a uniform surface without adhering to the polymerized gel. The hydrogel was then treated with the photo-activatable cross-linker, N-Sulfosuccinimidyl-6-(4′-azido-2′-nitrophenylamino) hexanoate (sulfo-SANPAH, Pierce, Rockford, IL), under UV irradiation to bind extracellular matrix to the surface. Activated PAG was coated with 0.2 mg/ml type I collagen (BD Bioscience, San Jose, CA) diluted in 0.2 N acetic acid for 6 h at 4°C. Stiff substrates were prepared by coating the same collagen I onto the glass slides. Before plating cells, substrates were soaked into medium and kept in the incubator for 30 min.

Immunofluorescence and live-cell confocal microscopy. After allowing cells to spread on stiff and soft substrates for 6 h, cells were fixed with 2% paraformaldehyde (Sigma-Aldrich) for 1 hour. Fixed cells were permeabilized with 0.1% Triton X-100 (Fisher biotech) for 10 min and blocked with PBS supplemented with FBS (10%, v/v) for 20 min to avoid non-specific binding. The following primary antibodies were used for immuno-staining: anti-vinculin antibody (Sigma) at 1:200, anti-FAK antibody (Santa Cruz Biotechnology, Santa Cruz, CA) at 1:50, anti-paxillin antibody (G.D. Longmore, Washington University in Saint Louis) at 1:100, anti-zyxin antibody (Sigma) at 1:100, and anti-phosphomyosin light chain 2 (Ser 19) antibody (Cell Signalling Technology, Bervely, MA) at 1:50. To detect phospho-specific FAK, anti-FAK (phospho Tyr397) antibody (Novus Biologicals) was used at 1:50. Actin filaments and nuclear DNA were stained using Alexa-Fluor phalloidin 488 (Invitrogen) and 300 nM DAPI (Invitrogen), respectively. In fixed specimen, fluorescent images of nuclei, actin filaments, and focal adhesions were collected using a Cascade 1 K CCD camera (Roper Scientific, Tucson, AZ) mounted on a fluorescence microscope (TE2000E, Nikon, Melville, NY) and equipped with a 60x Plan Fluor lens (N.A. 1.4).

3D visualization of fixed samples and monitoring of focal adhesion movements of RUBY-lifeact and EGFP-paxillin transfected cells were conducted with confocal laser microscopy (A1, Nikon) through a 60x plan lens or a 60x water immersion lens (N.A. 1.2). Each frame was taken every 4–5 min. Thanks to the use of low laser power, no significant photobleaching was observed over capture times of up to 6 h.

Fluorescence recovery after photobleaching (FRAP). FRAP experiments were carried out on a Nikon A1 confocal microscope using both the galvano and the resonant scanners, allowing for concurrent data collection and sample bleaching. By gradually lowering the plane of focus in EGFP-paxillin and RUBY-Lifeact transfected cells actin cap associated focal adhesions were distinguished from conventional focal adhesions. Right after that scan area was chosen to include an actin cap associated focal adhesion and a conventional focal adhesion. Outer half side of an individual focal adhesion was bleached simultaneously by a 405 nm laser set to 100% power and monitored using a Plan Apo 60x (N.A. 1.4) differential interference contrast oil immersion objective.

Data acquisition and statistical analysis. Images were analyzed and processed using MetaMorph (Molecular Devices, Downingtown, PA) and NIS elements (Nikon). Morphometric analysis (area, length, breadth, and shape factor) of focal adhesions was conducted by tracing them by hand. Images used in accessing light intensity (Figs. S4 and S5) were all obtained from the same specimen fixed and stained using identical primary and secondary antibodies and captured under the identical camera setting. Graphpad Prism (Graphpad Software, San Diego, CA) was used to calculate and plot mean and standard error of the mean (SEM) of measured quantities and significances were assessed by two-tailed unpaired t-tests or One-way ANOVA.

Computational interpretation. To understand how surface compliance affects focal adhesion size, we espouse the view that the size of focal adhesions is roughly proportional to the thickness of stress fibers. We justify this assumption by noting that force increases with the thickness of the stress fibers, and adhesion size also increases with applied force[27]. The model of Walcott and Sun (2010) predicts that stress fiber formation is a balance of surface compliance dependent aggregation of actin filaments and compliance-independent breakdown of stress fibers, which means large and stable fibers are formed in stiff substrate while only small and transient fibers are formed on soft substrates since formation of stress fibers is faster than breakdown in stiff substrates and vice versa. Therefore, this model predicts that stress fibers (and therefore adhesions) are smaller on soft substrates than on stiff ones. Consequently, if stiffness affects only the size distribution of stress fibers and not their number, then large focal adhesions are formed preferentially on stiff substrates, while small focal adhesions are relatively insensitive to substrate compliance (their frequency may even increase as substrate compliance increases). The stiffness insensitivity of the small adhesions arises because, at any stiffness, the majority of adhesions are small.

The following empirical equation is proposed that relates the probability of forming a stress fiber of size N, which is corresponding to the size of a focal adhesion to surface compliance, which is proportional to the inverse of the Young's modulus of the surface, E^{-1}):

$$P(E,N) = e^{-\alpha(E)(N-1)^{\beta}}$$

where β is a non-dimensional fitting parameter (β=3.3) and α is the function

$$\alpha = 34.7\left(45 + (k_{to}\tau)^{-1}\right)^{-1.9},$$

where k_{to} is the rate of actin fiber breakdown and τ is the time constant of stress fiber formation. This time constant is related to properties of non-muscle myosin II (isometric force, F_0, unloaded shortening rate, v_0, and c, a curve-fitting parameter in A.V. Hill's force-velocity relationship for muscle (Hill 1938)), the properties of cytoskeletal filaments (their length L and the viscous drag between them due to the action of cross-linking proteins, b^0_{Lin}), and the stiffness-dependent viscous drag between the adhesions and the surface ($b(E)$):

$$\tau = \frac{2cLb^0_{Lin}}{-(F_0 + v_0 b(E)) + \sqrt{(F_0 + v_0 b(E))^2 + 4b(E)v_0 F_0 c}}.$$

Finally, we may relate the viscous drag between the adhesions to the Young's modulus of the surface through the relation

$$b(E) = \frac{C\kappa E}{CE + 3\kappa} \frac{1}{k_d + k_a} \frac{k_a}{k_d}.$$

where k_d and k_a are the unloaded attachment and detachment rate of surface binding proteins, κ is the stiffness of these proteins and C is the circumference of the region over which the proteins apply load. Together, these equations provide a relationship between adhesion size, which we assume is proportional to thickness of stress fibers, and substrate compliance and allows us to understand why large adhesions such as actin cap associated focal adhesions are more sensitive to changes in surface compliance than small adhesions such as conventional focal adhesions.

1. Chan, C. E. & Odde, D. J. Traction dynamics of filopodia on compliant substrates. *Science* **322**, 1687–1691 (2008).
2. Pelham, R. J., Jr. & Wang, Y. Cell locomotion and focal adhesions are regulated by substrate flexibility. *Proc Natl Acad Sci U S A* **94**, 13661–13665 (1997).
3. Butcher, D. T., Alliston, T. & Weaver, V. M. A tense situation: forcing tumour progression. *Nat Rev Cancer* **9**, 108–122 (2009).
4. Engler, A. J., Sen, S., Sweeney, H. L. & Discher, D. E. Matrix elasticity directs cell lineage specification. *Cell* **126**, 677–689 (2006).
5. Wang, H. B., Dembo, M., Hanks, S. K. & Wang, Y. Focal adhesion kinase is involved in mechanosensing during fibroblast migration. *Proc Natl Acad Sci U S A* **98**, 11295–11300 (2001).
6. Wehrle-Haller, B. & Imhof, B. The inner lives of focal adhesions. *Trends Cell Biol* **12**, 382–389 (2002).
7. Schoenwaelder, S. M. & Burridge, K. Bidirectional signaling between the cytoskeleton and integrins. *Curr Opin Cell Biol* **11**, 274–286 (1999).
8. Burridge, K., Turner, C. E. & Romer, L. H. Tyrosine phosphorylation of paxillin and pp125FAK accompanies cell adhesion to extracellular matrix: a role in cytoskeletal assembly. *J Cell Biol* **119**, 893–903 (1992).
9. Turner, C. E., Glenney, J. R., Jr. & Burridge, K. Paxillin: a new vinculin-binding protein present in focal adhesions. *J Cell Biol* **111**, 1059–1068 (1990).
10. Hirota, T. *et al.* Zyxin, a regulator of actin filament assembly, targets the mitotic apparatus by interacting with h-warts/LATS1 tumor suppressor. *J Cell Biol* **149**, 1073–1086 (2000).
11. Gilmore, A. P. & Burridge, K. Regulation of vinculin binding to talin and actin by phosphatidyl-inositol-4-5-bisphosphate. *Nature* **381**, 531–535 (1996).
12. Calderwood, D. A. & Ginsberg, M. H. Talin forges the links between integrins and actin. *Nat Cell Biol* **5**, 694–697. (2003).
13. Otey, C. A., Pavalko, F. M. & Burridge, K. An interaction between alpha-actinin and the beta 1 integrin subunit in vitro. *J Cell Biol* **111**, 721–729. (1990).
14. Crawford, A. W., Michelsen, J. W. & Beckerle, M. C. An interaction between zyxin and alpha-actinin. *J Cell Biol* **116**, 1381–1393. (1992).
15. Critchley, D. R. in *Guidebook to the Cytoskeletal and Motor Proteins* (eds T. Kreis & R. Vale) 22–23 (Oxford University Press, 1993).
16. Geiger, B., Spatz, J. P. & Bershadsky, A. D. Environmental sensing through focal adhesions. *Nat Rev Mol Cell Biol* **10**, 21–33 (2009).
17. Sastry, S. K. & Burridge, K. Focal adhesions: a nexus for intracellular signaling and cytoskeletal dynamics. *Exp Cell Res* **261**, 25–36 (2000).
18. Khatau, S. B. *et al.* A perinuclear actin cap regulates nuclear shape. *Proc Natl Acad Sci U S A* **106**, 19017–19022 (2009).
19. Gay, O. *et al.* RefilinB (FAM101B) targets FilaminA to organize perinuclear actin networks and regulates nuclear shape. *Proc Natl Acad Sci U S A* **108**, 11464–11469 (2011).
20. Hotulainen, P. & Lappalainen, P. Stress fibers are generated by two distinct actin assembly mechanisms in motile cells. *J Cell Biol* **173**, 383–394 (2006).
21. Heath, J. P. & Holifield, B. F. On the mechanisms of cortical actin flow and its role in cytoskeletal organisation of fibroblasts. *Symp Soc Exp Biol* **47**, 35–56 (1993).
22. Small, J. V., Rottner, K., Kaverina, I. & Anderson, K. I. Assembling an actin cytoskeleton for cell attachment and movement. *Biochim Biophys Acta* **1404**, 271–281 (1998).

23. Razafsky, D. & Hodzic, D. Bringing KASH under the SUN: the many faces of nucleo-cytoskeletal connections. *J Cell Biol* **186**, 461–472 (2009).

24. Burnette, D. T. *et al.* A role for actin arcs in the leading-edge advance of migrating cells. *Nat Cell Biol* **13**, 371–381 (2011).

25. Mohl, C., Kirchgessner, N., Schafer, C., Hoffmann, B. & Merkel, R. Quantitative mapping of averaged focal adhesion dynamics in migrating cells by shape normalization. *Journal of cell science* **125**, 155–165, doi:10.1242/jcs.090746 (2012).

26. Diener, A. *et al.* Control of focal adhesion dynamics by material surface characteristics. *Biomaterials* **26**, 383–392, doi:10.1016/j.biomaterials.2004.02.038 (2005).

27. Riveline, D. *et al.* Focal contacts as mechanosensors: externally applied local mechanical force induces growth of focal contacts by an mDia1-dependent and ROCK-independent mechanism. *J Cell Biol* **153**, 1175–1186 (2001).

28. Pasapera, A. M., Schneider, I. C., Rericha, E., Schlaepfer, D. D. & Waterman, C. M. Myosin II activity regulates vinculin recruitment to focal adhesions through FAK-mediated paxillin phosphorylation. *J Cell Biol* **188**, 877–890 (2010).

29. Walcott, S. & Sun, S. X. A mechanical model of actin stress fiber formation and substrate elasticity sensing in adherent cells. *Proc Natl Acad Sci U S A* **107**, 7757–7762.

30. Lo, C. M., Wang, H. B., Dembo, M. & Wang, Y. L. Cell movement is guided by the rigidity of the substrate. *Biophys J* **79**, 144–152. (2000).

31. Nicolas, A., Geiger, B. & Safran, S. A. Cell mechanosensitivity controls the anisotropy of focal adhesions. *Proc Natl Acad Sci U S A* **101**, 12520–12525 (2004).

32. Yoshigi, M., Hoffman, L. M., Jensen, C. C., Yost, H. J. & Beckerle, M. C. Mechanical force mobilizes zyxin from focal adhesions to actin filaments and regulates cytoskeletal reinforcement. *J Cell Biol* **171**, 209–215 (2005).

33. Stewart-Hutchinson, P. J., Hale, C. M., Wirtz, D. & Hodzic, D. Structural requirements for the assembly of LINC complexes and their function in cellular mechanical stiffness. *Exp Cell Res* **314**, 1892–1905 (2008).

34. Lombardi, M. L. *et al.* The interaction between nesprins and sun proteins at the nuclear envelope is critical for force transmission between the nucleus and cytoskeleton. *J Biol Chem* **286**, 26743–26753 (2010).

35. Grashoff, C. *et al.* Measuring mechanical tension across vinculin reveals regulation of focal adhesion dynamics. *Nature* **466**, 263–266 (2011).

36. McBeath, R., Pirone, D. M., Nelson, C. M., Bhadriraju, K. & Chen, C. S. Cell shape, cytoskeletal tension, and RhoA regulate stem cell lineage commitment. *Dev Cell* **6**, 483–495 (2004).

37. Ngu, H. Effect of focal adhesion proteins on endothelial cell adhesion, motility and orientation response to cyclic strain. *Ann Biomed Eng* **38**, 208–222 (2010).

38. Buxboim, A., Ivanovska, I. L. & Discher, D. E. Matrix elasticity, cytoskeletal forces and physics of the nucleus: how deeply do cells 'feel' outside and in? *J Cell Sci* **123**, 297–308 (2010).

Acknowledgements

Author contributions

DHK, GDL, and DW designed the experiments and wrote the paper. DHK, SBH, GDL, and DW analyzed the data. YF and GDL provided new reagents. SW and SXS designed and conducted the computational analysis.

Additional information

Supplementary information accompanies this paper at http://www.nature.com/scientificreports

How to cite this article: Kim, D.-H. *et al.* Actin cap associated focal adhesions and their distinct role in cellular mechanosensing. *Sci. Rep.* **2**, 555; DOI:10.1038/srep00555 (2012).